JCTC Journal of Chemical Theory and Computation

Article

pubs.acs.org/JCTC

Excitation Energies with Cost-Reduced Variant of the Active-Space EOMCCSDT Method: The EOMCCSDt-$\bar{3}$ Approach

Han-Shi Hu and Karol Kowalski*

William R. Wiley Environmental Molecular Sciences Laboratory, Pacific Northwest National Laboratory, K8-91, P.O.Box 999, Richland, Washington 99352, United States

ABSTRACT: In this paper, we discuss the performance of several simplified variants of equation-of-motion coupled cluster method (EOMCC) with iterative inclusion of singles, doubles, and active-space triples (EOMCCSDt). In particular, we explore simplified EOMCCSDt approaches that enable one to generate the triply excited amplitudes in an on-the-fly manner. The original EOMCCSDt formulation has already demonstrated great success in encapsulating the most important excited-state correlation effects due to triples. In analogy to the original EOMCCSDT-3 formulation, the proposed approach can bypass the typical bottlenecks associated with the need for storing triply excited amplitudes. In this paper, we illustrate the performance of several approximate EOMCCSDt methods, named EOMCCSDt-$\bar{3}$ and EOMCCSDt-$\bar{3}$, on typical benchmark systems including C_2, N_2, ozone, ethene, and *E*-butadiene molecules. These new methods yield excitation energies close to the EOMCCSDt ones. The extrapolation of excitation energies for basis sets ranging from cc-pVDZ to cc-pV6Z for N_2 and C_2 shows very good convergence to the experimental results for states dominated by single excitations. The performance of the EOMCCSDt-$\bar{3}$x approach is also compared with the results obtained with popular CCSDR(3) and CC3 approaches.

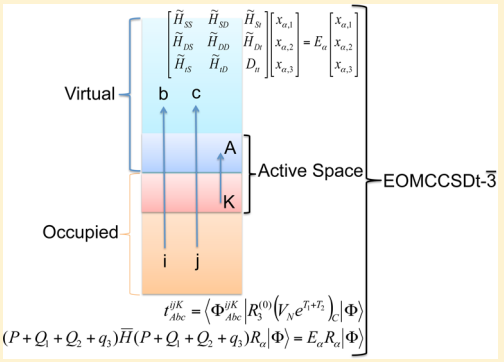

INTRODUCTION

The equation-of-motion coupled cluster (EOMCC) methods[1−6] or closely related linear response CC,[7−12] symmetry adapted cluster configuration interaction formalisms,[13] and spin-flip EOMCC methods[14] have evolved into one of the major tools for calculating vertical excitation energies (VEE) and for the characterization of excited-state potential energy surfaces. Over the last few decades, there has been significant effort toward establishing the hierarchy of various EOMCC approximations, which has enabled accurate descriptions of a wide spectrum of excited states characterized by various configurational structures of corresponding wave functions. For example, for relatively small systems, excited states dominated by single excitations can be very accurately described by the EOMCC approximation involving single and double excitations (EOMCCSD approach[1−3]). For more complicated states containing non-negligible contributions from doubly excited (with respect to the reference determinant) configurations, the inclusion of collective three-body excitations in the EOMCC formalism is required for accurate results. However, full inclusion of triply excited amplitudes in the EOMCC formalism (resulting in the EOMCCSDT formalism[15]) comes at a high numerical price, which is proportional to N^8, where N symbolically designates the system size. Several noniterative methods have been introduced with the purpose of mimicking the effect of triply excited amplitudes in calculating vertical excitation energies such as the EOMCCSD(T)[16] and EOMCCSD($\tilde{T}$)[17] formulations, several noniterative methods originating from various formalisms including linear response CC,[18] methods of moments of the CC equations (MMCC),[19−21] spin-flip formalism,[14,22,23] or perturbative techniques for similarity transformed Hamiltonian.[24−27]

Unfortunately, the conclusions about the EOMCC accuracies inferred from the benchmark calculations for small molecular systems cannot be directly extrapolated toward larger molecular assemblies. As shown in the series of papers discussing EOMCC calculations for singly excited states in molecules composed of several tens of light atoms,[28−31] the EOMCCSD approach for these systems no longer matches the level of accuracy of the EOMCCSD method for small systems. These studies clearly indicate a growing role of higher-rank excitations (three-body effects) in describing singly excited states of large systems. The importance of this higher-rank excitations was shown in refs 32−34. which have recently been reiterated in refs 27, 35, and 36 in studies of DNA bases. Although the noniterative EOMCC methods accounting for triple excitations in most cases improve the EOMCCSD results, the recent studies of $(TiO_2)_n$ clusters[37] pointed out possible problems of these noniterative formulations in describing singly excited states. In order to achieve agreement with experimentally inferred data, the iterative inclusion of the triple excitation was necessary. It was also demonstrated that active-space EOMCCSDT formulations (or EOMCCSDt for short)[15] provide an efficient way of attaining near-EOMCCSDT

Received: June 12, 2013
Published: September 27, 2013

accuracies. Given the growing interest in strongly correlated systems relevant to catalysis or photovoltaics, there is a natural need for iterative EOMCC methods capable of iterative inclusion of the triple excitations. The purpose of this paper is to discuss potential formulations that can meet this goal for systems composed of 300−800 orbitals, which are currently beyond the reach of existing EOMCC implementations with iterative triple excitations.

In this paper, we focus on the iterative variants of the EOMCCSDt methods, which employ a subset of the most important triply excited amplitudes relevant to a given state, offering in this way a significant reduction of the computational cost and memory demands associated with the full EOMCCSDT method. Special attention will be paid to the active-space formulation of the EOMCCSDT-3 type (for original EOMCCSDT-3 formulation, see refs 4 and 17), which offers a possibility of using computational drivers for noniterative methods, which have been recently tested in large scale calculations performed on leadership-class computer architectures.[28,30,31] In this work, on the other hand, we would like to provide the first numerical estimates of the EOMCCSDt-3 or more precisely EOMCCSDt-$\overline{3}$ accuracies for small benchmark systems such as the C_2, N_2, ozone, ethene (C_2H_4), and *E*-butadiene (C_4H_6) molecules for which either full configuration interaction (FCI) or EOMCCSDT results are available for comparison.

THEORY

Active-space CC methods have been introduced by Adamowicz, Oliphant, and Piecuch in a series of papers describing their theoretical and implementation aspects.[38−49] The tailored CC methods[50−52] are also based on the active-space CC ideas. Several recent studies[49,53] have shown great promise in utilizing these methods in ground-state calculations involving bond breaking and forming processes. The excited-state extension of the CCSDt methods based on the EOMCC framework, the active-space EOMCCSDT methods, have demonstrated great efficiency of active-space methods in encapsulating the most important excited-state correlation effects due to triples,[54] where various strategies employing various subsets of triply excited amplitudes have been studied. In recent studies, the CCSDt/EOMCCSDt ideas[49] have been integrated with the general method of moments CC framework[55] (see ref 49). The details of the active-space CC/EOMCC methods can be found in the cited literature.

The EOMCCSDt approach is composed of two steps. In the first step, the CCSDt ground-state wave function is parametrized as follows

$$|\Psi_0\rangle = e^{T_1+T_2+t_3}|\Phi\rangle \tag{1}$$

where

$$T_1 = \sum_{i,a} t_a^i X_a^+ X_i \tag{2}$$

$$T_2 = \sum_{\substack{i<j\\a<b}} t_{ab}^{ij} X_a^+ X_b^+ X_j X_i \tag{3}$$

$$t_3 = \sum_{\substack{i<j<K\\A<b<c}} t_{Abc}^{ijK} X_A^+ X_b^+ X_c^+ X_K X_j X_i \tag{4}$$

where X_p (X_p^+) represent annihilation (creation) operators of the electron in the *p*th single particle state, the indices *i*, *j*, *k*, ... (*a*, *b*, *c*, ...) refer to generic occupied (unoccupied) spin−orbital indices, and *K* (*A*) refer to occupied (unoccupied) active spin−orbital indices. The reference function $|\Phi\rangle$ is usually chosen as the Hartree−Fock (HF) Slater determinant. The amplitudes determining cluster operators (eqs 2−4) are obtained by solving the CC equations

$$\langle \Phi_i^a|\bar{H}|\Phi\rangle = 0 \qquad \forall_{i,a} \tag{5}$$

$$\langle \Phi_{ij}^{ab}|\bar{H}|\Phi\rangle = 0 \qquad \forall_{i<j;a<b} \tag{6}$$

$$\langle \Phi_{ijK}^{Abc}|\bar{H}|\Phi\rangle = 0 \qquad \forall_{i<j<K;A<b<c} \tag{7}$$

where the similarity transformed Hamiltonian $\bar{H}$ is defined as

$$\bar{H} = e^{-T_1-T_2-t_3} H e^{T_1+T_2+t_3} \tag{8}$$

and where $\langle\Phi_i^a|$, $\langle\Phi_{ij}^{ab}|$, $\langle\Phi_{ijK}^{Abc}|$, are the singly, doubly, and selected triply excited configurations defined with respect to the reference function, for example,

$$|\Phi_{ijK}^{Abc}\rangle = X_A^+ X_b^+ X_c^+ X_K X_j X_i|\Phi\rangle \tag{10}$$

The *H* operator in eq 8 designates the electronic Hamiltonian. Once the ground-state CCSDt problem is solved, the excited-state wave function for some αth state takes the following form:

$$|\Psi_\alpha\rangle = R_\alpha e^{T_1+T_2+t_3}|\Phi\rangle \tag{11}$$

where the excitation operator R_α for the EOMCCSDt approach is defined as

$$R_\alpha = R_{\alpha,0} + R_{\alpha,1} + R_{\alpha,2} + r_{\alpha,3} \tag{12}$$

where $R_{\alpha,0}$ is a scalar operator and

$$R_{\alpha,1} = \sum_{i,a} r_a^i(\alpha) X_a^+ X_i \tag{13}$$

$$R_{\alpha,2} = \sum_{\substack{i<j\\a<b}} r_{ab}^{ij}(\alpha) X_a^+ X_b^+ X_j X_i \tag{14}$$

$$r_{\alpha,3} = \sum_{\substack{i<j<K\\A<b<c}} r_{Abc}^{ijK}(\alpha) X_A^+ X_b^+ X_c^+ X_K X_j X_i \tag{15}$$

The amplitudes defining the R_α operator and the corresponding energy E_α are defined through the eigenvalue problem

$$(P + Q_1 + Q_2 + q_3)\bar{H}(P + Q_1 + Q_2 + q_3)R_\alpha|\Phi\rangle = E_\alpha R_\alpha|\Phi\rangle \tag{16}$$

where *P*, Q_1, Q_2, and q_3 are the projection operators onto the reference function, singly excited, doubly excited, and selected triply excited configurations, that is,

$$P = |\Phi\rangle\langle\Phi| \tag{17}$$

$$Q_1 = \sum_{i,a} |\Phi_i^a\rangle\langle\Phi_i^a| \tag{18}$$

$$Q_2 = \sum_{i<j;a<b} |\Phi_{ij}^{ab}\rangle\langle\Phi_{ij}^{ab}| \tag{19}$$

dx.doi.org/10.1021/ct400501z | J. Chem. Theory Comput. 2013, 9, 4761−4768

$$q_3 = \sum_{\substack{i<j<K \\ A<b<c}} |\Phi_{ijK}^{Abc}\rangle\langle\Phi_{ijK}^{Abc}| \tag{20}$$

With matrix notation, the eigenvalue can be represented as

$$\begin{bmatrix} E_{\mathrm{CCSDt}} & \bar{H}_{\mathrm{PS}} & \bar{H}_{\mathrm{PD}} & \bar{H}_{\mathrm{Pt}} \\ \bar{H}_{\mathrm{SP}} & \bar{H}_{\mathrm{SS}} & \bar{H}_{\mathrm{SD}} & \bar{H}_{\mathrm{St}} \\ \bar{H}_{\mathrm{DP}} & \bar{H}_{\mathrm{DS}} & \bar{H}_{\mathrm{DD}} & \bar{H}_{\mathrm{Dt}} \\ \bar{H}_{\mathrm{tP}} & \bar{H}_{\mathrm{tS}} & \bar{H}_{\mathrm{tD}} & \bar{H}_{\mathrm{tt}} \end{bmatrix} \begin{bmatrix} x_{\alpha,0} \\ x_{\alpha,1} \\ x_{\alpha,2} \\ x_{\alpha,3} \end{bmatrix} = E_\alpha \begin{bmatrix} x_{\alpha,0} \\ x_{\alpha,1} \\ x_{\alpha,2} \\ x_{\alpha,3} \end{bmatrix} \tag{21}$$

where $\bar{H}_{XY}$ (X,Y = P,S,D,t) are the blocks of the similarity transformed Hamiltonian matrix defined by eq 16. For example, $\bar{H}_{\mathrm{SP}} = Q_1\bar{H}P$, $\bar{H}_{\mathrm{SD}} = Q_1\bar{H}Q_2$, $\bar{H}_{\mathrm{tt}} = q_3\bar{H}q_3$, etc. Since the T_1, T_2, and t_3 operators satisfy the CCSDt eqs 5−7, the $\bar{H}_{\mathrm{SP}}$, $\bar{H}_{\mathrm{DP}}$, and $\bar{H}_{\mathrm{tP}}$ blocks are composed of zeros. In the above matrix representation of the EOMCCSDt approach, the E_{CCSDt} is the CCSDt ground-state energy, and vectors $x_{\alpha,0}$, $x_{\alpha,1}$, $x_{\alpha,2}$, and $x_{\alpha,3}$ are the vectors with the components corresponding to scalar, singly, doubly, and triply excited amplitudes of R_α operator, respectively. Because the CCSDt equations are satisfied, to determine energies E_α and corresponding vectors $x_{\alpha,1}$, $x_{\alpha,2}$, and $x_{\alpha,3}$, it is sufficient to diagonalize $\bar{H}$ in the $Q_1 + Q_2 + q_3$ space, that is,

$$\begin{bmatrix} \bar{H}_{\mathrm{SS}} & \bar{H}_{\mathrm{SD}} & \bar{H}_{\mathrm{St}} \\ \bar{H}_{\mathrm{DS}} & \bar{H}_{\mathrm{DD}} & \bar{H}_{\mathrm{Dt}} \\ \bar{H}_{\mathrm{tS}} & \bar{H}_{\mathrm{tD}} & \bar{H}_{\mathrm{tt}} \end{bmatrix} \begin{bmatrix} x_{\alpha,1} \\ x_{\alpha,2} \\ x_{\alpha,3} \end{bmatrix} = E_\alpha \begin{bmatrix} x_{\alpha,1} \\ x_{\alpha,2} \\ x_{\alpha,3} \end{bmatrix} \tag{22}$$

The main computational bottleneck of the EOMCCSDt method is the memory requirements associated with the storage of the $x_{\alpha,3}$ vector (or vectors when Davidson type procedures[56] are used to diagonalize matrix 22), which is proportional to $N_{\mathrm{o}}N_{\mathrm{u}}n_{\mathrm{o}}^2n_{\mathrm{u}}^2$, where N_{o}, N_{u}, n_{o}, and n_{u} refer to the number of occupied and unoccupied active spin−orbitals and occupied and unoccupied spin−orbitals, respectively. Similarly, the numerical overhead of the EOMCCSDt is proportional to $N_{\mathrm{o}}N_{\mathrm{u}}n_{\mathrm{o}}^2n_{\mathrm{u}}^4$. Although the numerical complexity of the EOMCCSDt method is significantly reduced with respect to the full EOMCCSDT formulation, for large systems described by several hundred of orbitals the above estimates still constitute a significant challenge.

In order to reduce the scaling of the EOMCCSDt approach even further, we will explore possibilities of on-the-fly generation of triply excited amplitudes, which eliminates the need for storing these objects in the iterative procedures. Our main goal is to simplify the CCSDt and EOMCCSDt equations in a way that enable one to express the t_{Abc}^{ijK} and $r_{Abc}^{ijk}(\alpha)$ as functions of the lower order amplitudes, that is, (t_a^i, t_{ab}^{ij}) and $(t_a^i, t_{ab}^{ij}), r_a^i(\alpha), r_{ab}^{ij}(\alpha)$, respectively. This can be achieved by combining the ideas behind the CCSDT-3 and EOMCCSDT-3 approaches and active-space methods.

In analogy to the CCSDT-3 formalisms, eqs 5 and 6 remain unchanged while the equations for triples, eq 7, are simplified to the form

$$\langle\Phi_{ijK}^{Abc}|F_{\mathrm{N}}t_3 + (V_{\mathrm{N}}\, \mathrm{e}^{T_1+T_2})_{\mathrm{C}}|\Phi\rangle = 0 \tag{23}$$

where F_{N} and V_{N} operators are one- and two-body components of the electronic Hamiltonian in normal product form H_{N} ($H_{\mathrm{N}} = H - \langle\Phi|H|\Phi\rangle = F_{\mathrm{N}} + V_{\mathrm{N}}$). Once HF orbitals are employed, the F_{N} operator can be represented in the diagonal form

$$F_{\mathrm{N}} = \sum_\lambda \varepsilon_\lambda N[X_\lambda^+ X_\lambda] \tag{24}$$

where ε's correspond to the HF orbital energies and symbol N designates a normal product of corresponding operators. Taking advantage of eqs 23 and 24, the t_{Abc}^{ijK} amplitudes are given by the equation

$$t_{Abc}^{ijK} = \langle\Phi_{ijK}^{Abc}|R_3^{(0)}(V_{\mathrm{N}}\, \mathrm{e}^{T_1+T_2})_{\mathrm{C}}|\Phi\rangle \tag{25}$$

where $R_3^{(0)}$ is three body zeroth-order resolvent operator defined as

$$R_3^{(0)} = \sum_{\substack{i<j<k \\ a<b<c}} \frac{|\Phi_{ijk}^{abc}\rangle\langle\Phi_{ijk}^{abc}|}{\varepsilon_i + \varepsilon_j + \varepsilon_k - \varepsilon_a - \varepsilon_b - \varepsilon_c} \tag{26}$$

Equations 5, 6, and 23 define the CCSDt-3 equations.

As in the linear response CC theory,[7−12] the equations determining excited-state energies and related R_α operators can be obtained through the diagonalization of the Jacobian matrix corresponding to the CCSDt-3 equations. However, in order to avoid calculating costly contributions to the Jacobian matrix stemming from the t_{Abc}^{ijK} -dependent terms, we approximate Jacobian matrix by terms depending on singly and doubly excited cluster amplitudes obtained in CCSDt-3 calculations. This leads to the following eigenvalue problem, which will henceforth be referred to as the EOMCCSDt-$\bar{3}$ approximation

$$\begin{bmatrix} \tilde{H}_{\mathrm{SS}} & \tilde{H}_{\mathrm{SD}} & \tilde{H}_{\mathrm{St}} \\ \tilde{H}_{\mathrm{DS}} & \tilde{H}_{\mathrm{DD}} & \tilde{H}_{\mathrm{Dt}} \\ \tilde{H}_{\mathrm{tS}} & \tilde{H}_{\mathrm{tD}} & D_{\mathrm{tt}} \end{bmatrix} \begin{bmatrix} x_{\alpha,1} \\ x_{\alpha,2} \\ x_{\alpha,3} \end{bmatrix} = E_\alpha \begin{bmatrix} x_{\alpha,1} \\ x_{\alpha,2} \\ x_{\alpha,3} \end{bmatrix} \tag{27}$$

where diagonal block D_{tt} is defined by corresponding differences of orbital energies $(\varepsilon_A + \varepsilon_b + \varepsilon_c - \varepsilon_i - \varepsilon_j - \varepsilon_K)$ and $\tilde{H}_{XY}$ designate the corresponding block of the similarity transformed Hamiltonian $\tilde{H}$ defined as

$$\tilde{H} = \mathrm{e}^{-T_1-T_2} H\, \mathrm{e}^{T_1+T_2} \tag{28}$$

To explore the role of the neglected t_{Abc}^{ijK}-dependent terms in EOMCCSDt matrix 22 on the accuracy of the calculated excitation energies, we also consider a test approximation (referred to as the EOMCCSDt-$\bar{3}$x approach) given by the eigenvalue problem

$$\begin{bmatrix} \bar{H}_{\mathrm{SS}} & \bar{H}_{\mathrm{SD}} & \bar{H}_{\mathrm{St}} \\ \bar{H}_{\mathrm{DS}} & \bar{H}_{\mathrm{DD}} & \bar{H}_{\mathrm{Dt}} \\ \bar{H}_{\mathrm{tS}} & \bar{H}_{\mathrm{tD}} & D_{\mathrm{tt}} \end{bmatrix} \begin{bmatrix} x_{\alpha,1} \\ x_{\alpha,2} \\ x_{\alpha,3} \end{bmatrix} = E_\alpha \begin{bmatrix} x_{\alpha,1} \\ x_{\alpha,2} \\ x_{\alpha,3} \end{bmatrix} \tag{29}$$

In contrast to the EOMCCSDt-$\bar{3}$ approximation, in the EOMCCSDt-$\bar{3}$x method, calculating $r_{Abc}^{ijK}(\alpha)$ amplitudes on-the-fly requires $(t_a^i, t_{ab}^{ij}, r_a^i(\alpha), r_{ab}^{ij}(\alpha))$ as well as perturbative t_{Abc}^{ijK} given by eq 25. For this reason EOMCCSDt-$\bar{3}$x is more expensive than the EOMCCSDt-$\bar{3}$ formalism.

COMPUTATIONAL DETAILS

The EOMCCSDt-$\bar{3}$ codes have been developed based on the existing Tensor Contraction Engine (TCE)[57] implementations of the EOMCCSDt approach[54] in NWChem.[58] For testing purposes, we used the version of the EOMCCSDt-$\bar{3}$ code that stores t_3 and $r_{3,\alpha}$ amplitudes instead of generating them on the fly; effort toward the development of economical implementation of the EOMCCSDt-$\bar{3}$ method utilizing on-the-fly

dx.doi.org/10.1021/ct400501z | J. Chem. Theory Comput. 2013, 9, 4761−4768

generation of triply excited amplitudes is in progress. For this reason in this paper, we focus entirely on small benchmark systems for which FCI or full EOMCCSDT results are available. To denote the active-space used in the EOMCCSDt calculations, we invoked (N_o, N_u) notation where N_o and N_u stand for the number of occupied and unoccupied active orbitals, respectively. For all systems considered here, notation N_o and N_v refer to highest-lying occupied and lowest-lying virtual orbitals. In all calculations, core electrons were kept frozen.

NUMERICAL EXAMPLES

In this section, we discuss a few examples illustrating the performance of the EOMCCSDt-$\bar{3}$ method and its EOMCCSDt-$\bar{3}$x variant in the calculations for vertical excitation energies (VEE) in the N_2, C_2, O_3, ethene, and *E*-butadiene molecules. These results are compared with VEEs obtained with other methods including EOMCCSD, EOMCCSDt, CCSDR(3),[59] CC2[60] and CC3[61] (for ethene and *E*-butadiene), EOMCCSDT, and FCI (N_2, C_2, and ozone), as well as with the available experimental data. In all EOMCCSDt-$\bar{3}$ and EOMCCSDt-$\bar{3}$x calculations, we used the ground-state restricted HF determinant as a reference for the EOMCC calculations.

For N_2, C_2, and ozone molecules, the best approximation to the full ground-state CCSDT energies is provided by the CCSD(T) approach (see Table 1) with corresponding errors not exceeding 2 mhartree (for O_3 and N_2 systems these differences are as small as 0.5 and 0.08 mhartree, respectively). The CCSDt energies are invariably located above the CCSDT results. The largest difference between CCSDt and CCSDT results can be observed for the O_3 molecule (13 mhartree). For all systems discussed here, the ground-state CCSDt-3 energies are only slightly different from the CCSDt ones and provide significant improvements of the ground-state CCSD energies.

Table 1. The Ground-State Energies (in hartree) Obtained with the CCSD,CCSDt-3, CCSDt, CCSD(T), and CCSDT Methods for C_2, N_2 and O_3 Benchmark Systems[a]

	C_2	N_2	O_3
CCSD	−75.700 61	−109.263 06	−224.959 38
CCSDt-3	−75.715 45	−109.271 28	−224.979 45
CCSDt	−75.718 06	−109.272 16	−224.981 90
CCSD(T)	−75.728 35	−109.274 82	−224.995 43
CCSDT	−75.726 94	−109.274 90	−224.994 94

[a]The calculations for the C_2, N_2, and O_3 were performed employing modified aug-cc-pVDZ, cc-pVTZ, and POL1 basis sets, respectively.

A. Excitation Energies for N_2. For the N_2 molecule, we have performed a series of EOMCC calculations for the low-lying singlet states: $1^1\Sigma_u^-$, $1^1\Delta_u$, $1^1\Pi_g$, and $1^1\Pi_u$, which have been previously studied with high-level EOMCC methods. While the $1^1\Sigma_u^-$, $1^1\Delta_u$, and $1^1\Pi_g$ states are dominated by single excitations, the $1^1\Pi_u$ state has a partially biexcited character (see ref 62 for details of configurational structure of the FCI wave function). In Table 2.1, we have listed the calculated values of VEEs for the cc-pVDZ basis set. One can notice that for singly excited states $1^1\Sigma_u^-$, $1^1\Delta_u$, and $1^1\Pi_g$, the EOMCCSDt-$\bar{3}$, EOMCCSDt-$\bar{3}$x, and EOMCCSDt methods provide very good approximations to the full EOMCCSDT results. For the $1^1\Pi_u$ state with doubly excited components, the EOMCCSDt VEE is located very close to the EOMCCSDT value, while the EOMCCSDt-$\bar{3}$ and EOMCCSDt-$\bar{3}$x VEEs are located 0.15 and 0.18 eV above the EOMCCSDT value. This indicates that for states with doubly excited components, the proper inclusion of EOMCCSDt-$\bar{3}$x significantly improves the EOMCCSD excitation energy for the $1^1\Pi_u$ state. Table 2.2 contains the EOMCCSD, EOMCCSDt-$\bar{3}$, and EOMCCSDt-$\bar{3}$x VEEs obtained for cc-pV*X*Z (*X* = D,T,Q,5,6) basis sets. For the largest basis set employed (cc-pV6Z) containing 280 basis set functions, the EOMCCSDt-$\bar{3}$ approach provides a good approximation to the experimentally observed values. Similar conclusions can be made for the EOMCCSDt-$\bar{3}$x approach, which provides the results of the same quality as the

Table 2.2. A Comparison of the EOMCCSD, EOMCCSDt-$\bar{3}$,[a] and EOMCCSDt-$\bar{3}$x[a] VEEs of N_2 Obtained with Five Types of Basis Sets Ranging from cc-pVDZ to cc-pV6Z and the Experimental Data[b]

state	cc-pVDZ	cc-pVTZ	cc-pVQZ	cc-pV5Z	cc-pV6Z	expt[c]
			EOMCCSD			
$1^1\Sigma_u^-$	10.46	10.19	10.13	10.11	10.11	9.92
$1^1\Delta_u$	10.90	10.64	10.57	10.55	10.54	10.27
$1^1\Pi_g$	9.66	9.56	9.52	9.50	9.50	9.31
$1^1\Pi_u$	14.01	13.82	13.74	13.69	13.67	12.78
			EOMCCSt-$\bar{3}$			
$1^1\Sigma_u^-$	10.32	10.05	10.00	9.97	9.97	9.92
$1^1\Delta_u$	10.71	10.47	10.40	10.38	10.37	10.27
$1^1\Pi_g$	9.61	9.51	9.47	9.45	9.45	9.31
$1^1\Pi_u$	13.81	13.61	13.54	13.50	13.49	12.78
			EOMCCSDt-$\bar{3}$x			
$1^1\Sigma_u^-$	10.36	10.11	10.05	10.03	10.02	9.92
$1^1\Delta_u$	10.77	10.53	10.47	10.43	10.42	10.27
$1^1\Pi_g$	9.65	9.55	9.51	9.49	9.49	9.31
$1^1\Pi_u$	13.84	13.65	13.57	13.53	13.52	12.78
N_b[d]	28	60	110	182	280	

[a]Active space of (3,3) has been used in active space EOMCC calculations. [b]The calculated and experimental values of VEEs are reported in eV. [c]From experimental data of ref 69. [d]N_b represents the number of the basis set functions.

Table 2.1. A Comparison of VEEs (in eV) for the Low-Lying Excited States of N_2[a] Obtained with Various EOMCC, FCI Methods, And Experimental Results[b]

state	EOMSD	EOMSDt-$\bar{3}$[c]	EOMSDt-$\bar{3}$x[c]	EOMSDt[c]	EOMSDT[d]	FCI[d]	expt[e]
$1^1\Sigma_u^-$	10.46	10.32	10.36	10.33	10.33	10.33	9.92
$1^1\Delta_u$	10.90	10.71	10.77	10.72	10.73	10.72	10.27
$1^1\Pi_g$	9.66	9.61	9.65	9.60	9.59	9.58	9.31
$1^1\Pi_u$	14.01	13.81	13.84	13.67	13.66	13.61	12.78

[a]The equilibrium bond length in N_2 is 2.068 bohr.[68] [b]The cc-pVDZ basis set was used in all calculations. [c]Active space of (3,3) has been used in active space EOMCC calculation. [d]From ref 68. [e]From experimental data of ref 69.

Table 3.1. The EOMCCSD, EOMCCSDt-$\bar{3}$, EOMCCSDt-$\bar{3}$x, EOMCCSDt,[a] EOMCCSDT, and FCI VEEs (in eV) of C_2[b] Obtained with the Modified aug-cc-pVDZ Basis Set[70]

state	EOMCCSD	EOMCCSDt-$\bar{3}$	EOMCCSDt-$\bar{3}x$	EOMCCSDt	EOMCCSDT[c]	FCI[c]
$^1\Pi_u$	1.47	1.23	1.32	1.34	1.42	1.385
$^1\Delta_g$	4.35	2.99	2.99	2.58	2.70	2.293
$^1\Pi_g$	6.20	4.99	4.98	4.57	4.58	4.494
$^1\Sigma_u^+$	5.80	5.56	5.68	5.69	5.72	5.602

[a]In active-space EOMCCSDt calculations, a (2,4) active space was employed. [b]The equilibrium bond length in C_2 is 2.348 bohr.[68] [c]From ref 68.

EOMCCSDt-$\bar{3}$ method. This shows that for N_2 the inclusion of the T_3 clusters in the similarity transformed Hamiltonian plays a less important role. It is also instructive to compare the EOMCCSD and EOMCCSDt-$\bar{3}$ results for the cc-pV6Z basis set. For the lowest $1^1\Sigma_u^-$ state the EOMCCSD/cc-pV6Z results are characterized by 0.19 eV of error with respect to the experiment (9.92 eV), which is comparable to 0.05 eV of error produced by the EOMCCSDt-$\bar{3}$ approach. For the challenging $1^1\Pi_u$ state, the errors of the EOMCCSDt-$\bar{3}$ methods are significantly bigger (0.71 eV for the cc-pV6Z basis set). These errors can be attributed to oversimplified form of the triples−triples block of the similarity transformed Hamiltonian.

B. Excitation energies of C_2. The C_2 molecule provides an example of a system where the excited states are dominated by double excitations. Among the $1^1\Pi_u$, $1^1\Delta_g$, $1^1\Pi_g$, and $1^1\Sigma_u^+$ states studied here, the $1^1\Delta_g$ and $1^1\Pi_g$ states are dominated by double excitations. The remaining two states, $1^1\Pi_u$ and $1^1\Sigma_u^+$, are predominantly singly excited. It is well-known that for doubly excited states the EOMCCSD cannot provide an accurate prediction of the corresponding VEEs. This situation is illustrated by the EOMCC results in Table 3.1. obtained with the modified aug-cc-pVDZ basis set of ref 63. For the doubly excited states $1^1\Delta_g$ and $1^1\Pi_g$, the EOMCCSD discrepancies with respect to the FCI results are as big as 2.1 and 1.7 eV, respectively. The inclusion of triple excitations improves the situation by reducing the EOMCCSD errors to 0.4 and 0.1 eV. The full EOMCCSDt results for $1^1\Delta_g$ and $1^1\Pi_g$ states are very close to the EOMCCSDT ones with differences not exceeding 0.12 eV. The corresponding errors for the EOMCCSDt-$\bar{3}$ and EOMCCSDt-$\bar{3}$x methods for doubly excited states are bigger and amount to 0.7 and 0.5 eV. Also, the EOMCCSDt-$\bar{3}$ and EOMCCSDt-$\bar{3}$x results are very close (the largest difference of 0.12 eV occurs for the Σ_u^+ state; for the remaining states the differences are smaller than 0.1 eV). The results shown in Table 3.1 also demonstrate the general trend of active-space methods to underestimate the EOMCCSDT predictions. For example, the EOMCCSDt-$\bar{3}$ VEE for the $1^1\Pi_u$ state is located 0.19 eV below the EOMCCSDT VEE. This behavior may be a specific feature of the basis set employed.

As in the case of N_2 system, we also explore the performance of the EOMCCSDt-$\bar{3}$ methods in the limit of very large basis sets. For this purpose, we performed a series of EOMCCSD, EOMCCSDt-$\bar{3}$, and EOMCCSDt-$\bar{3}$x calculations for cc-pVXZ (X = D,T,Q,5,6) basis sets. The results are shown in Table 3.2. In analogy to the N_2 system, the cc-pV6Z EOMCCSDt-$\bar{3}$ results for singly excited states ($1^1\Pi_u$ and $1^1\Sigma_u^+$) are in very good agreement with the experiment. For example, for the $1^1\Pi_u$, a value of 1.07 eV obtained with the EOMCCSDt-$\bar{3}$ approach agrees well with the experimentally inferred value of 1.04 eV. For doubly excited states the accuracies of the EOMCCSDt-$\bar{3}$ worsens. For $1^1\Pi_g$ state, the cc-pV6Z EOMCCSDt-$\bar{3}$ VEE estimate is 4.82 eV, which is 0.57 eV above the experimental value (4.25 eV). However, 4.82 eV

Table 3.2. A Comparison of the EOMCCSD, EOMCCSDt-$\bar{3}$,[a] and EOMCCSDt-$\bar{3}$x,[a] VEEs of C_2 Obtained with Five Basis Sets Ranging from cc-pVDZ to cc-pV6Z[b]

state	cc-pVDZ	cc-pVTZ	cc-pVQZ	cc-pV5Z	cc-pV6Z	expt[c]
			EOMCCSD			
$^1\Pi_u$	1.52	1.33	1.30	1.30	1.30	1.04
$^1\Delta_g$	4.60	4.81	4.89	4.92	4.92	
$^1\Pi_g$	6.35	6.49	6.53	6.54	6.54	4.25
$^1\Sigma_u^+$	5.91	5.62	5.56	5.55	5.55	5.36
			EOMCCSDt-$\bar{3}$			
$^1\Pi_u$	1.32	1.13	1.10	1.08	1.07	1.04
$^1\Delta_g$	3.42	3.29	3.24	3.20	2.85	
$^1\Pi_g$	5.17	4.96	4.89	4.85	4.82	4.25
$^1\Sigma_u^+$	5.67	5.39	5.34	5.32	5.31	5.36
			EOMCCSDt-$\bar{3}$x			
$^1\Pi_u$	1.44	1.26	1.23	1.20	1.18	1.04
$^1\Delta_g$	3.43	3.29	3.25	3.20	2.86	
$^1\Pi_g$	5.17	4.96	4.89	4.85	4.82	4.25
$^1\Sigma_u^+$	5.82	5.55	5.50	5.47	5.45	5.36
N_b[d]	28	60	110	182	280	

[a]Active space of (2,4) has been used in active space EOMCC calculation. [b]The calculated and experimental values of VEEs are reported in eV. [c]From experimental data of ref 71. [d]N_b represents the number of the basis set functions.

compares favorably with the corresponding EOMCCSD value of 6.54 eV. As for the N_2 system the EOMCCSDt-$\bar{3}$x predictions are only slightly different than the EOMCCSDt-$\bar{3}$ ones.

In Figure 1, we show the CC/EOMCC potential energy surfaces (PESs) corresponding to the ground ($1^1\Sigma_g^+$) and first excited singlet state ($1^1\Pi_u$). For the nuclear geometries considered in Figure 1 (1.0−3.0 Å), the CCSDt-3/EOMCCSDt-$\bar{3}$ results are virtually parallel to the CCSDT/EOMCCSDT ones. This can be best seen for the elongated C−C bond, where the CCSD/EOMCCSD energies start to significantly differ from the CCSDT/EOMCCSDT ones. It is worth noticing that the CCSDt-3/EOMCCSDt-$\bar{3}$ PESs reflect all the topological features of the CCSDT/EOMCCSDT curves including the crossings between $1^1\Sigma_g^+$ and $1^1\Pi_u$ curves as well as the relative separations between corresponding PESs. Although as shown in ref 64, the right description of PES for C_2 requires quadruply excited clusters to be included, our aim in this report however is to demonstrate that the CCSDt-3/EOMCCSDt-$\bar{3}$ results are closely following the CCSDT/EOMCCSDT results.

C. Singlet Excitations in the Ozone Molecule. Because of the strong correlation effects in the ground state and the existence of complicated excited states dominated by double excitations, the ozone molecule has been frequently used in studies employing various high-level CC approaches.[65] As far as the singlet excited states are concerned, the biggest challenge is

dx.doi.org/10.1021/ct400501z | J. Chem. Theory Comput. 2013, 9, 4761−4768

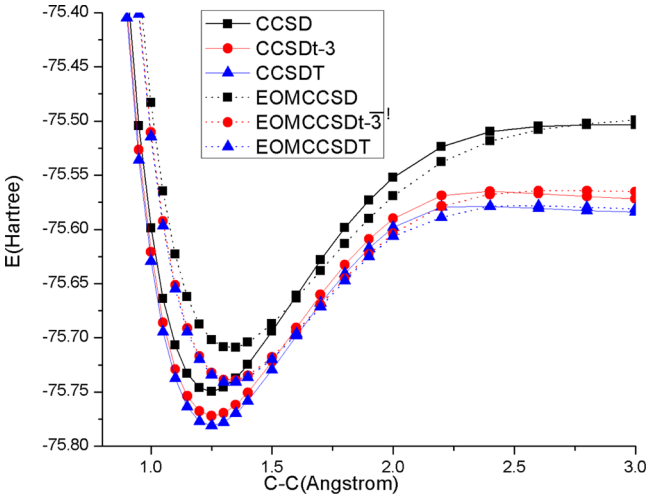

Figure 1. The CC/EOMCC potential energy curves for the $1^1\Sigma_g^+$ and $1^1\Pi_u$ states of C_2. All calculations have been performed with the modified aug-cc-pVDZ basis set.

posed by the doubly excited 2^1A_1 state dominated by double excitations.

It is well-known that for the POL1 basis set, the EOMCCSD method places this state as a third excited state of $^1A_1$ symmetry, which is a common feature of the EOMCCSD approach when applied to description of doubly excited states.[19,66] As seen from Table 4, the full inclusion of triples (EOMCCSDT) lowers the EOMCCSD 2^1A_1 excitation energy, 9.82 eV, by 4.73 eV (EOMCCSDT VEE is equal to 5.09 eV). At the same time, the EOMCCSDt result (4.95 eV) is in good agreement with the full EOMCCSDT value. As an effect of approximating the triples−triples block of the similarity transformed Hamiltonian, both EOMCCSDt-$\bar{3}$ and EOMCCSDt-$\bar{3}$x results (5.81 and 5.82 eV, respectively) are placed around 0.7 eV above the EOMCCSDT values. Given the cost reduction offered by the EOMCCSDt-$\bar{3}$ method and poor quality of the EOMCCSD result for the 2^1A_1 state, the performance of the EOMCCSDt-$\bar{3}$ is satisfactory. For the remaining singlet states (1^1A_2, 1^1B_1, 1^1B_2) the EOMCCSDt-$\bar{3}$ results are almost of the EOMCCSDT quality. The bigger discrepancies can be found for the 1^1B_2 state where the EOMCCSDt-$\bar{3}$ value of 5.07 eV is in a good agreement with the experimental data. For this state inspection of the EOMCCSDt-$\bar{3}$x result (5.25 eV vs 5.28 eV obtained with the EOMCCSDT method) shows that the inclusion of the T_3 amplitudes in the $\bar{H}$ operator plays an important role in recovering the EOMCCSDT level of accuracy by the EOMCCSDt-$\bar{3}$ methods. This effect is likely due to the strong correlation effect in the ground state.

D. Singlet Excitations in Ethene and *E*-Butadiene. In Tables 5 and 6, we provide a comparison between EOMCCSD, EOMCCSDt-$\bar{3}$, and EOMCCSDT calculations for ethene and *E*-butadiene performed in POL1 and aug-cc-pVTZ (ethene only) basis sets. The equilibrium geometries of ethene and *E*-butadiene were obtained by MP2/6-31G* optimization to be consistent with literature from which the CC3 and CCSDR(3) VEEs were taken.[67] The assignment of irreducible representations for particular excited states corresponds to the convention employed by NWChem. From Table 5 one can see that the EOMCCSD and EOMCCSDT calculations employing POL1 basis set can reproduce the corresponding EOMCC results obtained with the larger aug-cc-pVTZ basis set. The (1,7) active space for the ethane molecule has been defined based on the leading EOMCCSD amplitudes. This is a very efficient way of defining minimum-size active space, which does not lead to a significant loss of accuracy. All POL1 EOMCCSDt-$\bar{3}$ results reported in Table 5 are very close to the EOMCCSDT ones with errors (with respect to the EOMCCSDT approach) not exceeding 0.07 eV (1^1A_g state). Similar situation can be observed for the aug-cc-pVTZ basis set (although the corresponding errors are slightly bigger than for the POL1 basis set). It should be also stressed that for both basis sets the

Table 5. Vertical Excitation Energies (in eV) of C_2H_4 Are Calculated by EOMCCSD and EOMCCSDt-$\bar{3}$ with Basis Sets of POL1 and aug-cc-pVTZ, Respectively

	POL1			aug-cc-pVTZ		
C_2H_4	SD	SDt-$\bar{3}$(1,7)	SDT	SD	SDt-$\bar{3}$(1,7)	SDT
2^1A_g	8.79	8.70	8.76	8.84	8.69	8.79
1^1A_u	9.21	9.12	9.19	9.26	9.11	9.22
1^1B_{1g}	9.65	9.63	9.61	9.77	9.73	9.70
1^1B_{1u}	7.31	7.23	7.28	7.40	7.28	7.35
1^1B_{2g}	7.98	7.91	7.96	8.06	7.95	8.02
1^1B_{2u} $\pi \rightarrow \pi^*$[a]	8.01	7.92	7.92	8.00	7.89	7.90
1^1B_{3g}	8.02	7.94	7.98	8.12	7.99	8.06
1^1B_{3u}	9.99	10.00	9.95	10.47	10.42	10.40

[a]Here $^1B_{2u}$ state corresponds to the $^1B_{1u}$ state in literature, which represents the $\pi \rightarrow \pi^*$ excitation.

Table 6. Vertical Excitation Energies (in eV) of C_4H_6 Calculated by EOMCCSD, EOMCCSDt-$\bar{3}$, and EOMCCSDT with Basis Set of POL1

C_4H_6	SD	SDt-$\bar{3}$(1,9)	SDt-$\bar{3}$(2,8)	SDt-$\bar{3}$(2,9)	SDT
2^1A_g	7.03	6.78	6.85	6.74	6.52
1^1A_u	6.60	6.56	6.49	6.52	6.57
1^1B_g	6.29	6.24	6.18	6.20	6.26
1^1B_u	6.34	6.26	6.24	6.24	6.23

Table 4. The EOMCC Vertical Excitation Energies (in eV) for the O_3 Molecule[a] Calculated with the Sadlej pVTZ Basis Sets (POL1)[72] Employing the (5,1) Active Space

state	E_{EOMSD}	$E_{EOMSDt\text{-}\bar{3}}$	$E_{EOMSDt\text{-}\bar{3}x}$	E_{EOMSDt}	E_{EOMSDT}[b]	expt[b]
2^1A_1	9.82	5.81	5.82	4.95	5.09	3.45−4.02[c]
1^1A_2	2.30	2.17	2.26	2.16	2.17	1.62[d]; 1.92[e]
1^1B_1	2.36	2.24	2.32	2.23	2.25	2.1[d]
1^1B_2	5.39	5.07	5.25	5.28	5.28	4.86[d]

[a]The equilibrium bond length and bond angle in O_3 are R_{O-O} = 2.40373 bohr and α_{O-O-O} = 116.8°.[73] [b]From ref 73. [c]From ref 74. [d]From ref 75. [e]From ref 76.

dx.doi.org/10.1021/ct400501z | J. Chem. Theory Comput. 2013, 9, 4761−4768

Table 7. Vertical Excitation Energies (in eV) of C_2H_4 and *E*-C_4H_6 Calculated by CC2, CCSDR(3) and CC3 Methods (aug-cc-pVTZ Basis Set) as well as Experimental Data

		CC2[67]	CCSDR(3)[67]	CC3[67]	EOMSD	EOMSDt-$\bar{3}$	expt
C_2H_4	1^1B_{1u}	7.90	7.87	7.89	8.00	7.89	7.60[67]
E-C_4H_6	1^1B_{1u}	6.13	6.19		6.33	6.22	6.25,[77] 5.92[78]
	2^1A_g	7.06	6.82	6.63	7.09	6.90	

EOMCCSDt-$\bar{3}$ results have tendency to slightly underestimate the EOMCCSDT excitation energies.

As in the case of ethane, for *E*-butadiene the choice of the active space based on the largest EOMCCSD amplitudes enabled us to define (2,9) model space, which provides a reasonable trade-off between numerical cost and accuracy. From the results shown in Table 6, one can see that for the 1^1A_u, 1^1B_g, and 1^1B_u states, the POL1 EOMCCSDt-$\bar{3}$ results are slightly below EOMCCSDT ones with errors not exceeding 0.06 eV. A more interesting situation occurs for the 2^1A_g state where the discrepancy between EOMCCSD and EOMCCSDT results is as big as 0.5 eV. The EOMCCSDt-$\bar{3}$ approach using relatively small active space is capable of reducing this error to 0.22 eV.

Based on the results available in the literature, for the C_2H_4 and C_4H_6 systems, we were able to make a comparison between EOMCCSDt-$\bar{3}$ results and results obtained with other methods accounting for triple excitations (CCSDR(3) and CC3 methods). For the 1^1B_{1u} state, the EOMCCSDt-$\bar{3}$ verical excitation energy (see Table 7) is virtually identical to the results obtained with the CCSDR(3) and CC3 methods. For C_4H_6, the EOMCCSDt-$\bar{3}$ VEEs for 1^1B_{1u} and 2^1A_g states are in good agreement with the CCSDR(3) results. The CC3 excitation energy for the 2^1A_g state of *E*-butadiene differs by 0.19 and 0.27 eV with the VEEs obtained with CCSDR(3) and EOMCCSDt-$\bar{3}$, respectively.

CONCLUSIONS

We have derived two simplified variants of the active-space EOMCCSDt approaches: EOMCCSDt-$\bar{3}$ and EOMCCSDt-$\bar{3}$x, which can bypass the typical bottlenecks of the memory requirement associated with the storage of the triple vectors in the iterative procedures by generating the triply excited amplitudes in an on-the-fly manner, which reduces the $N_oN_un_o^2n_u^4$ scaling of EOMCCSDt to $N_oN_un_o^2n_u^3$ (or, to be more concise, to the maximum value between $N_oN_un_o^2n_u^3$ and $n_o^2n_u^4$). Next, we have performed comprehensive investigations of the performance of these methods for the typical benchmark systems including C_2, N_2, and O_3 molecules. First, the vertical excitation energies (VEEs) were obtained together with other methods including EOMCCSD, EOMCCSDt, EOMCCSDT, and FCI, as well as with the available experimental data at the ground state equilibrium geometries of C_2, N_2, and O_3 molecules, which shows that EOMCCSDt-$\bar{3}$, EOMCCSDt-$\bar{3}$x, and EOMCCSDt methods provide very good approximations to the full EOMCCSDT method for excited states dominated by single excitations. For states with doubly excited components, EOMCCSDt-$\bar{3}$ and EOMCCSDt-$\bar{3}$x significantly improve the EOMCCSD excitation energies, though the EOMCCSDt VEEs are closer to the EOMCCSDT ones for most cases. Second, five types of basis sets cc-pV*X*Z (*X* = D,T,Q,5,6) have been employed to obtain the VEEs by EOMCCSD, EOMCCSDt-$\bar{3}$, and EOMCCSDt-$\bar{3}$x methods. For the largest basis set employed (cc-pV6Z) containing 280 basis set functions, the EOMCCSDt-$\bar{3}$ and EOMCCSDt-$\bar{3}$x approaches provide good agreement with the experimentally observed values. This is not the case for the EOMCCSD approach. Third, we have also computed the CC/EOMCC potential energy surfaces corresponding to the ground ($1^1\Sigma_g^+$) and first excited singlet state ($1^1\Pi_u$) of C_2 with C−C bond length ranging from 1.0 to 3.0 Å, showing that the CCSDt-3/EOMCCSDt-$\bar{3}$ PESs reflect all the topological features of the CCSDT/EOMCCSDT curves while the CCSD/EOMCCSD energies significantly differ from the CCSDT/EOMCCSDT ones. Our calculations for ethane and *E*-butadiene also show that the EOMCCSDt-$\bar{3}$ results are in a good agreement with the results obtained with the CCSDR(3) approach. There is ongoing effort in our group to derive the parallel version of these methods in an on-the-fly manner to enable studies of larger systems with basis set number of around 300−800.

AUTHOR INFORMATION

Corresponding Author

*E-mail: karol.kowalski@pnl.gov.

Notes

The authors declare no competing financial interest.

ACKNOWLEDGMENTS

H.S.H. acknowledges Dr. Kiran Bhaskaran-Nair for helpful discussion and Dr. Kenneth Lopata for helpful proof reading of the manuscript. This work was supported by the Extreme Scale Computing Initiative (H.S.H., K.K.), a Laboratory Directed Research and Development Program at Pacific Northwest National Laboratory. All calculations have been performed using EMSL, a national scientific user facility sponsored by the Department of Energy's Office of Biological and Environmental Research and located at Pacific Northwest National Laboratory. The Pacific Northwest National Laboratory is operated for the U.S. Department of Energy by the Battelle Memorial Institute under Contract No. DE-AC06-76RLO-1830.

REFERENCES

(1) Geertsen, J.; Rittby, M.; Bartlett, R. J. *Chem. Phys. Lett.* **1989**, *164*, 57−62.
(2) Comeau, D. C.; Bartlett, R. J. *Chem. Phys. Lett.* **1993**, *207*, 414−423.
(3) Stanton, J. F.; Bartlett, R. J. *J. Chem. Phys.* **1993**, *98*, 7029−7039.
(4) Watts, J. D.; Gwaltney, S. R.; Bartlett, R. J. *J. Chem. Phys.* **1996**, *105*, 6979−6988.
(5) Stanton, J. F.; Gauss, J. *J. Chem. Phys.* **1996**, *104*, 9859−9869.
(6) Del Bene, J. E.; Watts, J. D.; Bartlett, R. J. *J. Chem. Phys.* **1997**, *106*, 6051−6060.
(7) Monkhorst, H. J. *Int. J. Quantum Chem., Symp.* **1977**, *11*, 421−432.
(8) Sekino, H.; Bartlett, R. J. *Int. J. Quantum Chem., Symp.* **1984**, *18*, 255−265.
(9) Dalgaard, E.; Monkhorst, H. J. *Phys. Rev. A* **1983**, *28*, 1217−1222.
(10) Takahashi, M.; Paldus, J. *J. Chem. Phys.* **1986**, *85*, 1486−1501.
(11) Koch, H.; Jørgensen, P. *J. Chem. Phys.* **1990**, *93*, 3333−3344.
(12) Koch, H.; Jensen, H. J. Aa.; Jørgensen, P.; Helgaker, T. *J. Chem. Phys.* **1990**, *93*, 3345−3350.

(13) (a) Nakatsuji, H. *Chem. Phys. Lett.* **1978**, *59*, 362−364. (b) Nakatsuji, H. *Chem. Phys. Lett.* **1979**, *67*, 329−333. (c) Nakatsuji, H. *Chem. Phys. Lett.* **1991**, *177*, 331−337. (d) Nakatsuji, H.; Ehara, M. *J. Chem. Phys.* **1993**, *98*, 7179−7184.
(14) Krylov, A. I. *Chem. Phys. Lett.* **2001**, *338*, 375−384.
(15) Kowalski, K.; Piecuch, P. *J. Chem. Phys.* **2001**, *115*, 643−651.
(16) Watts, J. D.; Bartlett, R. J. *Chem. Phys. Lett.* **1995**, *233*, 81−87.
(17) Watts, J. D.; Bartlett, R. J. *Chem. Phys. Lett.* **1996**, *258*, 581−588.
(18) Christiansen, O.; Koch, H.; Jørgensen, P. *J. Chem. Phys.* **1996**, *105*, 1451−1459.
(19) Kowalski, K.; Piecuch, P. *J. Chem. Phys.* **2004**, *120*, 1715−1738.
(20) Wloch, M.; Lodriguito, M. D.; Piecuch, P.; Gour, J. R. *Mol. Phys.* **2006**, *104*, 2149−2172.
(21) Piecuch, P.; Gour, J. R.; Wloch, M. *Int. J. Quantum Chem.* **2009**, *109*, 3268−3304.
(22) Krylov, A. I. *Chem. Phys. Lett.* **2001**, *350*, 522−530.
(23) Manohar, P. U.; Krylov, A. I. *J. Chem. Phys.* **2008**, *129*, No. 194105.
(24) Hirata, S.; Nooijen, M.; Grabowski, I.; Bartlett, R. J. *J. Chem. Phys.* **2001**, *114*, 3919−3928.
(25) Hirata, S.; Nooijen, M.; Grabowski, I.; Bartlett, R. J. *J. Chem. Phys.* **2001**, *115*, 3967−3968.
(26) Shiozaki, T.; Hirao, K.; Hirata, S. *J. Chem. Phys.* **2007**, *126*, No. 244106.
(27) Watson, T. J., Jr.; Lotrich, V. F.; Szalay, P. G.; Perera, A.; Bartlett, R. J. *J. Phys. Chem. A* **2013**, *117*, 2569−2579.
(28) Kowalski, K.; Krishnamoorthy, S.; Villa, O.; Hammond, J. R.; Govind, N. *J. Chem. Phys.* **2010**, *132*, No. 154103.
(29) Glaesemann, K. R.; Govind, N.; Krishnamoorthy, S.; Kowalski, K. *J. Phys. Chem. A* **2010**, *114*, 8764−8771.
(30) Kowalski, K.; Olson, R. M.; Krishnamoorthy, S.; Aprà, E. *J. Chem. Theory Comput.* **2011**, *7*, 2200−2208.
(31) Lopata, K.; Reslan, R.; Kowalska, M.; Neuhauser, D.; Govind, N.; Kowalski, K. *J. Chem. Theory Comput.* **2011**, *7*, 3686−3693.
(32) Coussan, S.; Ferro, Y.; Trivella, A.; Rajzmann, M.; Roubin, P.; Wieczorek, R.; Manca, C.; Piecuch, P.; Kowalski, K.; Włoch, M.; Kucharski, S. A.; Musiał, M. *J. Phys. Chem. A* **2006**, *110*, 3920−3926.
(33) Valiev, M.; Kowalski, K. *J. Chem. Phys.* **2006**, *125*, No. 211101.
(34) Epifanovsky, E.; Kowalski, K.; Fan, P. D.; Valiev, M.; Matsika, S.; Krylov, A. I. *J. Phys. Chem. A* **2008**, *112*, 9983−9992.
(35) Szalay, P. G.; Watson, T.; Perera, A.; Lotrich, V. F.; Bartlett, R. J. *J. Phys. Chem. A* **2012**, *116*, 6702−6710.
(36) Szalay, P. G.; Watson, T.; Perera, A.; Lotrich, V. F.; Fogarasi, G.; Bartlett, R. J. *J. Phys. Chem. A* **2012**, *116*, 8851−8860.
(37) Berardo, E.; Hu, H.-S.; Kowalski, K.; Zwijnenburg, M. A. *J. Chem. Phys.* **2013**, *139*, No. 064313.
(38) Oliphant, N.; Adamowicz, L. *J. Chem. Phys.* **1991**, *94*, 1229−1235.
(39) Oliphant, N.; Adamowicz, L. *Int. Rev. Phys. Chem.* **1993**, *12*, 339−362.
(40) Piecuch, P.; Oliphant, N.; Adamowicz, L. *J. Chem. Phys.* **1993**, *99*, 1875−1900.
(41) Ivanov, V. V.; Adamowicz, L. *J. Chem. Phys.* **2000**, *112*, 9258−9268.
(42) Lyakh, D. I.; Ivanov, V. V.; Adamowicz, L. *Theor. Chem. Acc.* **2006**, *116*, 427−433.
(43) Lyakh, D. I.; Ivanov, V. V.; Adamowicz, L. *Mol. Phys.* **2007**, *105*, 1335−1357.
(44) Lyakh, D. I.; Ivanov, V. V.; Adamowicz, L. *J. Chem. Phys.* **2008**, *128*, No. 074101.
(45) Ivanov, V. V.; Lyakh, D. I.; Adamowicz, L. J. *Phys. Chem. Chem. Phys.* **2009**, *11*, 2355−2370.
(46) Piecuch, P.; Kucharski, S. A.; Bartlett, R. J. *J. Chem. Phys.* **1999**, *110*, 6103−6122.
(47) Piecuch, P. *Mol. Phys.* **2010**, *108*, 2987−3015.
(48) Shen, J.; Piecuch, P. *Chem. Phys.* **2012**, *401*, 180−202.
(49) Shen, J.; Piecuch, P. *J. Chem. Theory Comput.* **2012**, *8*, 4968−4988.
(50) Kinoshita, T.; Hino, O.; Bartlett, R. J. *J. Chem. Phys.* **2005**, *123*, No. 074106.
(51) Hino, O.; Kinoshita, T.; Chan, G. K.; Bartlett, R. J. *J. Chem. Phys.* **2006**, *124*, No. 114311.
(52) Melnichuk, A.; Bartlett, R. J. *J. Chem. Phys.* **2012**, *137*, No. 214103.
(53) Yang, K. R.; Jalan, A.; Green, W. H.; Truhlar, D. G. *J. Chem. Theory Comput.* **2013**, *9*, 418−431.
(54) Kowalski, K.; Hirata, S.; Wloch, M.; Piecuch, P.; Windus, T. L. *J. Chem. Phys.* **2005**, *123*, No. 074319.
(55) Kowalski, K.; Piecuch, P. *J. Chem. Phys.* **2001**, *115*, 2966−2978.
(56) Davidson, E. R. *Comput. Phys. Commun.* **1989**, *53*, 49−60.
(57) Hirata, S. *J. Phys. Chem. A* **2003**, *107*, 9887−9897.
(58) Valiev, M.; Bylaska, E. J.; Govind, N.; Kowalski, K.; Straatsma, T. P.; van Dam, H. J. J.; Wang, D.; Nieplocha, J.; Apra, E.; Windus, T. L.; de Jong, W. A. *Comput. Phys. Commun.* **2010**, *181*, 1477−1489.
(59) Christiansen, O.; Koch, H.; Jørgensen, P. *J. Chem. Phys.* **1996**, *105*, 1451.
(60) Christiansen, O.; Koch, H.; Jørgensen, P. *Chem. Phys. Lett.* **1995**, *243*, 409.
(61) Christiansen, O.; Koch, H.; Jørgensen, P.; Olsen, J. *J. Chem. Phys.* **1995**, *103*, 7429−7441.
(62) Christiansen, O.; Koch, H.; Jørgensen, P.; Olsen, J. *Chem. Phys. Lett.* **1996**, *256*, 185−194.
(63) Dunning, T. H. *J. Chem. Phys.* **1989**, *90*, 1007−1023.
(64) Li, X.; Gour, J. R.; Paldus, J.; Piecuch, P. *Chem. Phys. Lett.* **2008**, *461*, 321−326.
(65) Bhaskaran-Nair, K.; Kowalski, K. *J. Chem. Phys.* **2012**, *137*, No. 216101.
(66) Watts, J. D.; Bartlett, R. J. *Spectrochim. Acta A* **1999**, *55*, 495−507.
(67) Silva-Junior, M. R.; Sauer, S. P. A.; Schreiber, M.; Thiel, W. *Mol. Phys.* **2010**, *108*, 453−465.
(68) Kowalski, K.; Piecuch, P. *J. Chem. Phys.* **2004**, *120*, 1715−1738.
(69) Oddershede, J.; Grüner, N. E.; Diercksen, G. H. F. *Chem. Phys.* **1985**, *97*, 303−310.
(70) Kowalski, K. *J. Chem. Phys.* **2006**, *125*, No. 124101.
(71) Huber, K. P.; Herzberg, G. *Constants of Diatomic Molecules*; Van Nostrand: Princeton, 1979.
(72) Sadlej, A. J. *Collect. Czech. Chem. Commun.* **1988**, *53*, 1995−2016.
(73) Bhaskaran-Nair, K.; Kowalski, K. *J. Chem. Phys.* **2012**, *137*, No. 216101.
(74) Katayama, D. H. *J. Chem. Phys.* **1979**, *71*, 815−820.
(75) Anderson, S. M.; Morton, J.; Mauersberger, K. *J. Chem. Phys.* **1990**, *93*, 3826−3832.
(76) Thunemann, K.-H.; Peyerimhoff, S. D.; Buenker, R. J. *J. Mol. Spectrosc.* **1978**, *70*, 432−448.
(77) McDiarmid, R. *Chem. Phys. Lett.* **1992**, *188*, 423−426.
(78) McDiarmid, R. *J. Chem. Phys.* **1976**, *64*, 514.